Molecular evidence for the paraphyly of Scolecophidia and its evolutionary implications

AURÉLIEN MIRALLES* (iD), JULIE MARIN*, DAMIEN MARKUS*, ANTHONY HERREL†,
S. BLAIR HEDGES‡ & NICOLAS VIDAL*

*Institut de Systématique, Evolution, Biodiversité, Muséum national d'Histoire naturelle, CNRS UPMC EPHE, Sorbonne Universités, Paris, France
†Département Adaptations du vivant, UMR 7179 C.N.R.S/M.N.H.N., Paris, France
‡Center for Biodiversity, Temple University, Philadelphia, Pennsylvania

Abstract

The phylogenetic relationships between the three main clades of worm snakes remain controversial. This question is, however, crucial to elucidate the origin of the successful snake radiation, as these burrowing and miniaturized wormlike organisms represent the earliest branching clades within the snake tree. The present molecular phylogenetic study, intended to minimize the amount of missing data, provides fully resolved inter-subfamilial relationships among Typhlopidae. It also brings robust evidence that worm snakes (Scolecophidia) are paraphyletic, with the scolecophidian family Anomalepididae recovered with strong support as sister clade to the 'typical snakes' (Alethinophidia). Ancestral state reconstructions applied to three different traits strongly associated to a burrowing life-style (scolecoidy, absence of retinal cones and microstomy) provide results in favour of a burrowing origin of snakes, and suggest that worm snakes might be the only extant fossorial representatives of the primordial snake incursion towards an underground environment.

Introduction

Snakes are the most species-rich squamate clade, numbering more than 3600 extant species (Uetz *et al.*, 2018). They have traditionally been divided into two main groups: (1) The burrowing scolecophidians ('worm snakes') are miniaturized and microphthalmic snakes with a limited gape size, and feed on small prey (mainly ants and termites) on a frequent basis. (2) The alethinophidians ('typical snakes') are more ecologically diverse and most species feed on relatively large prey (primarily vertebrates) and do so less frequently (Greene, 1997; Cundall & Greene, 2000).

Due to their secretive habits and small size, worm snakes have long been neglected, although several recent higher-level studies have brought new insights into their systematics and evolutionary history (Adalsteinsson *et al.*, 2009; Vidal *et al.*, 2010; Hedges *et al.*,

Correspondence: Aurélien Miralles, Institut de Systématique, Evolution, Biodiversité, Muséum national d'Histoire naturelle, CNRS UPMC EPHE, Sorbonne Universités, CP30, 25 rue Cuvier 75005 Paris, Paris, France.
Tel.: +331 71 21 46 55; fax: +33 1 40 79 37 73; e-mail: miralles.skink@gmail.com

2014; Pyron & Wallach, 2014; Nagy *et al.*, 2015). They are now known to be of Gondwanan origin, and five main clades have been identified and recognised as family rank categories: Anomalepididae, Leptotyphlopidae, Typhlopidae, Gerrhopilidae and Xenotyphlopidae, the last two families having been described recently (Adalsteinsson *et al.*, 2009; Vidal *et al.*, 2010).

On the other hand, the relationships between the three main clades of worm snakes, Anomalepididae, Leptotyphlopidae and Typhlopoidea (which is subdivided into Gerrhopilidae, Xenotyphlopidae and Typhlopidae), remain controversial (e.g. Pyron *et al.*, 2013; Hsiang *et al.*, 2015; Reeder *et al.*, 2015; Figueroa *et al.*, 2016; Streicher & Wiens, 2016; Zheng & Wiens, 2016; Harrington & Reeder, 2017). This point is of particular significance as the phylogenetic status of worm snakes has bearings on the origin of snakes. Strictly burrowing squamates such as dibamids and amphisbaenians are distantly related to snakes, which form a group named Toxicofera together with anguimorphs and iguanians, both of epigean origin (Vidal & Hedges, 2005). However, among snakes, fossoriality (active

burrowing) is not only found in scolecophidians. It also characterizes two alethinophidian clades, the Aniliidae and the Uropeltoidea (Anomochilidae, Cylindrophiidae, Uropeltidae). Interestingly, both these taxa are devoid of the macrostomate (large mouth) anatomy present in all other alethinophidian snakes which permits the ingestion of very large prey.

Taking advantage of a multilocus molecular dataset intended to minimize the amount of missing data, the aims of the present study are the following: (1) to resolve the deepest node of the snake phylogenetic tree in general (and among the Typhlopidae in particular) and, (2) based on the newly inferred topology, to discuss the origin of extant snakes, thanks to ancestral state reconstructions focusing on the evolution of a set of traits characterizing the peculiar worm-snake morphotype.

Material and methods

Nomenclatural background and terminology

The generic classification of scolecophidians is based on Hedges *et al.* (2014) and Nagy *et al.* (2015) for Typhlopidae, Xenotyphlopidae and Gerrhopilidae, on Adalsteinsson *et al.* (2009) for Leptotyphlopidae, and on McDiarmid *et al.* (1999) for Anomalepididae. Based on our results, (1) 'Scolecophidia *sensu stricto*' will be used here to refer to the monophyletic unit containing all the Scolecophidia *sensu lato*, to the exclusion of the Anomalepididae, and (2)'Macrostomata *sensu stricto*' will refer to the monophyletic unit containing all the Macrostomata *sensu lato* (Vidal & Hedges, 2002), to the exclusion of the Tropidophiidae. It is worthwhile to emphasize here the distinction between the strictly nomenclatural term 'Macrostomata *sensu stricto*' which is used to refer to a clade, from the term 'macrostomy' or 'macrostomatan condition' (large mouth), which refers to an anatomical-functional state (see Cundall & Greene, 2000) having previously been hypothesized to represent a complex assemblage of exclusive synapomorphies for the Macrostomata *sensu lato* (Rieppel *et al.*, 2002; Longrich *et al.*, 2012) and which is opposed to the plesiomorphic 'microstomatan condition' (small mouth).

Sampling

Our sampling was specifically designed to investigate the deepest relationships among the snake evolutionary tree, ensuring it was exhaustive at the family level of the diversity encountered among the microstomatan snakes. Sampling also focused on the scolecophidian snakes, with genera selected to represent each of the five main clades (i.e. the families Anomalepididae, Gerrhopilidae, Leptotyphlopidae, Typhlopidae and Xenotyphlopidae) consensually recognized by the most recent phylogenetic studies focusing on this group (Vidal *et al.*, 2010; Hedges *et al.*, 2014; Nagy *et al.*, 2015).

More specifically, sampling efforts were made within Typhlopidae in order to resolve the deepest relationships within the family: our sampling contains representatives of 16 of the 18 genera of Typhlopidae recognized in Hedges *et al.* (2014), with at least one sample per genus. Only two monospecific genera (*Grypotyphlops* and *Cyclotyphlops*) are not represented as tissue sample of these rare taxa were not available. In most of our phylogenetic analyses, a few supraspecific terminal taxa (n = 6) represent chimeric assemblages of distinct species having unambiguously been demonstrated to form monophyletic units when compared to the other taxa sampled (e.g. *Rena*, which is a combination of sequences of *R. humilis* and *R. dulcis*, or *Epictia* which combines both *E. magnamaculata* and *E. columbi*, see Appendix S1 for more details). Previous studies have emphasized the positive contribution of composite taxa in phylogeny reconstruction, without influence on dating results, as long as the species used to build chimeras are known to form a monophyletic group to the exclusion of the other species in the dataset (Springer *et al.*, 2004; Poux *et al.*, 2006). Varanidae, Iguanidae and Lacertidae were used as hierarchical outgroups, respectively representing these major clades of Squamates: Anguimorpha, Iguania and Laterata.

We made an effort to ensure a dense coverage across the whole set of loci involved, in order to minimize the amount of missing data. This methodological issue has indeed been frequently emphasized by several squamate phylogenetic studies recently published (e.g. 81% of missing data in Pyron *et al.*, 2013 or 92% in Zheng & Wiens, 2016).

To overcome this issue, we followed a two step process. We first looked for available sequences in GenBank and selected the most informative markers. Then we sequenced the selected markers for missing taxa in order to minimize the amount of gaps in the matrix. Our final dataset contains a total of 14 nuclear loci : CAND1 (Cullin-Associated NEDD8-Dissociated protein 1), CMOS (Oocyte Maturation factor), DNAH3 (Dynein axonemal heavy chain 3), ENC1 (Ectodermal-Neural Cortex 1), SLC8A1 (Solute Carrier Family 8 Member 1), SNCAIP (Alpha-Synuclein-Interacting Protein), R35 (35 G protein-coupled receptor 149), ZEB2 (Zinc Finger E-Box Binding Homeobox 2), ZFP36 (Zinc Finger Protein 36), BDNF (Brain-Derived Neurotrophic Factor), RAG1 (Recombination activating gene 1), BMP2 (Bone morphogenetic protein 2), NT3 (Neurotrophin-3) and AMEL (Amelogenin).

The resulting matrix contains 43 taxa and a total of 9195 characters. In total, 190 new DNA sequences were generated and combined with previously published DNA sequences (mostly by Vidal *et al.*, 2010 and Wiens *et al.*, 2012), therefore representing a dense coverage across the whole set of loci involved, with only 11%

missing sequences (541 sequences out of a theoretical total of 602, *cf.* Appendix S1) and 17.2% missing data calculated on a nucleotide basis. For analyses excluding heterospecific chimeric assemblages, the dataset contains 13.1% missing sequences and 20.5% missing nucleotides).

Molecular procedure

DNA extraction was performed with the DNeasy Tissue Kit (Qiagen). Amplification and sequencing was performed using primers listed in Appendix S2. The DNA amplification was performed by polymerase chain reaction (PCR) in a final 21-μL volume containing 1 μL of dimethyl sulphoxide, 0.8 μL of dNTP 6.6 mM, 0.12 μL of Taq DNA polymerase, using 2.5 μL of the buffer provided by the manufacturer (100 units mL^{-1}) and 0.32 μL of each of the two primers at 10 pM. Finally, 1 μL of DNA extract was added. The PCR reactions were performed with the following conditions: initial denaturation at 94°C for 3 min, followed by 39 cycles (3 min at 94°C, 40 s at 47-55°C according to the primer pairs (Appendix S2), 1 min at 72°C) and a final elongation at 72°C for 10 min. Amplification products were visualized on ethidium bromide-stained agarose gels. The successfully amplified products were purified using the ExoSAP-IT purification kit according to the manufacturer's instruction. Sequencing was performed in both forward and reverse directions at Eurofins Scientific, a private company. All DNA sequences were assembled into contigs, edited and checked for errors using CodonCode Aligner (v. 2.0.6, CodonCode Corporation). No stop codons were found in protein coding genes. Strict individual consensus sequences were constructed by coding any sites found to be polymorphic using the corresponding IUPAC ambiguity codes. Sequence alignment was performed manually with MEGA7 (Kumar *et al.* 2016) using the alignment of Reeder *et al.* (2015) as a framework. With the exception of a 12 base pair long fragment removed from the CMOS dataset using Gblocks (Talavera & Castresana, 2007) with less stringent settings (smaller final blocks, gap position within the final blocks and less strict flanking position allowed), this task was straightforward. In all analyses, gaps were treated as missing data. All newly determined sequences were deposited in GenBank under accession numbers KY628461 to KY628650.

Phylogenetic inferences

Two approaches were used to infer phylogenetic relationships with a concatenated multilocus dataset. Bayesian inferences (BI) were performed with MrBayes [on XSDE, via CIPRES portal V3.1version 1.1.1], version 3.2.6 (Ronquist & Huelsenbeck, 2003) and Maximum likelihood (ML) analyses were performed with RAxML,

version 8 [HPC2 on XSEDE] (Stamatakis, 2014), both provided online by the CIPRES portal V3.1 (Miller *et al.*, 2010). The best-fit partition scheme for the combined dataset was selected with PartitionFinder 2.1.1 [on XSEDE] (Lanfear *et al.*, 2016), using the Bayesian Information Criterion. Branch lengths were linked across partitions. The set of potential substitution models was restricted to the GTR+G model (RAxML applies only the GTR +G and GTR+I+G models, and only GTR+G is recommended by the developer of RAxML given the potential interaction between I and G parameters). The greedy search option was used in PartitionFinder. The best-fit partitioning scheme divided the data into three partitions (by codon position). Bayesian analyses were performed by running 20 000 000 generations in four chains, saving the current tree every 100 generations. Four runs were performed and effective sample size (ESS) values for the combined parameter files were checked with Tracer, version 1.6 (Rambaut *et al.*, 2014), to ensure good mixing and convergence.

We used the MrBayes default burn-in (25%) and used the last 150 000 trees to construct a 50% majority rule consensus tree. For ML analyses, we performed 1000 bootstrap replicates to obtain a bootstrap majority rule consensus tree. Partition strategies by gene and codon position were also applied for both methods and resulted in similar results, both in terms of topologies and robustness (data not shown). Moreover, to ensure the absence of artefactual effects caused by the presence of chimeric assemblages, complementary BI and ML analyses were performed with strictly monospecific terminal taxa only.

Finally, separate ML analyses were also conducted for each of the 14 loci, taking into consideration that the recovery of congruent topologies from independent datasets (in this case, unlinked loci) represents a relevant criterion to assess clade reliability (Li & Lecointre, 2009). Along the same lines, a species tree (ST) was inferred with ASTRAL (Mirarab *et al.*, 2014; Sayyari & Mirarab, 2016) based on 14 complementary ML gene trees restricted to the same specific terminal taxa (in order to discard any chimeric assemblage from the resulting ST). Trees were visualized with FIGTREE, version 1.3.1 (http://tree.bio.ed.ac.uk/software/figtree/) and redrawn with Adobe Illustrator.

Dating

We estimated divergence times using BEAST v. 1.8.3. (Drummond *et al.*, 2012). The xml file was created using BEAUTi (v. 1.8.3.) (Drummond *et al.*, 2012) with the following parameters: unlinked substitution and clock models; GTR+G+I for each of the 14 genes; relaxed uncorrelated lognormal clock; a birth–death process to model speciation events; 50 million generations with sampling every 1000 steps. The RAxML tree

was used as the input tree (i.e. starting tree). We constrained the monophyly of the five calibrated nodes, of the clade excluding Lacertidae and *Anolis*, and of the clade excluding Lacertidae. All these constrained nodes were highly supported in both BI and ML phylogenetic analyses; the remaining relationships were estimated along with the divergence times.

We estimated node ages using a set of five calibration points which correspond to (1) the split between Afrophidia and Amerophidia, constrained at 105.8 Ma according to Vidal *et al.* (2009) and geological data (opening of the Atlantic Ocean) with a normal prior distribution (mean=105.8 and SD = 5) and (2) the root of the tree was set at a maximum of 200 Ma (i.e. Triassic-Jurassic boundary, as it approximately corresponds to the age of the squamate root, cf. review in Zheng & Wiens, 2016). The next two calibrations were maxima corresponding to geologic dates when the West Indian islands became habitable (rose above sea-level), namely (3) the node uniting all West Indian taxa (*Cubatyphlops caymanensis*, *C. anchaurus*, *Typhlops jamaicensis* and *Antillotyphlops catapontus*), constrained at a maximum of 37.2 Ma (Iturralde-Vinent & MacPhee, 1999), and (4) the node uniting the two *Mitophis* species (restricted to South Island of Hispaniola), constrained at a maximum of 10 Ma (Huebeck & Mann, 1985). Finally, (5) in the absence of available fossil or geological calibration, the extreme of the 95% credibility interval of the node time (highest posterior density interval, HPD) were used to constrain the split between *Anilios unguirostris* and *A. kimberleyensis* at a maximum of 21 Ma according to Marin *et al.* (2013). We assigned uniform prior distributions to the four latter nodes with a minimum of 0 Ma.

Analyses of character evolution

To investigate the evolutionary origins of the extant snakes, Ancestral State Reconstructions (ASR) were performed on our newly inferred topology. The evolution of three different binary morphological traits (presence/absence) characterizing an extreme subterranean life were reconstructed. All the reconstructed traits are obviously expected to be correlated. Nevertheless, they are not identically distributed among extant snakes, and may therefore contribute in offering different perspectives on the evolution of fossoriality in snakes. More specifically, these analyses were intended to determine, in the light of the newly inferred topology, whether the very peculiar morphology and ecology characterizing worm snakes is a derived trait, or if on the contrary, they constitute a conserved ecomorphotype inherited from the common ancestor of the extant snakes (subsequently lost in the Alethinophidia).

ASR based on the newly inferred topology was run using methods based on three different approaches (parsimony [MP-ASR], likelihood [ML-ASR] and Bayesian [BI-ASR] methods). Additionally, in order to assess the robustness of our reconstruction hypotheses, we ran a fourth kind of analysis taking into account topological uncertainty [BT-ASR]. The states of the characters were based on the literature and are presented in Appendix S3. Both the MP-ASR (with default parameters) and ML-ASR algorithms (with one-parameter Markov k-state (MK1) model algorithm (the asymmetrical 2-parameter Markov k-state model has also been tested and reconstructed similar ancestral states, not shown) were implemented in Mesquite v.3.11 (Maddison & Maddison, 2016). BI-ASR was conducted with the program BEAST v2.4.7 (Bouckaert *et al.*, 2014). We used the same parameters (substitution and clock models, number of generations) as for the timing analyses, and we fixed the topology using the RAxML topology.

The complementary BT-ASR taking into account tree topology uncertainty was performed with BayesTraits v2.0.2 (Pagel *et al.*, 2004) and run using the Bayesian implementation of the Multistate method for 10 million of generations (burn-in of 1 million). Exponential priors were seeded from a uniform hyperprior on the intervals of 0–13 for Macrostomy, 0–2 for Scolecoidy and 0-16 for Visual Cells, based on preliminary analyses exploring a range of values. Convergence of runs was assessed using Tracer v1.6 to ensure that analyses had reached stationarity and that ESS values for all parameters were above 200. We ensured that the prior means did not appear truncated which would indicate that the hyperprior distribution chosen was too narrow (Pagel & Meade, 2006). Analyses were run on a sample of the last 5000 trees from the combined post-burn-in posterior distributions of the phylogenetic BI independent runs.

The evolution of the following three traits was studied:

1) *Scolecoidy* [two states: *scolecoidy* versus *nonscolecoidy*]. The concept of scolecoidy ('resembling a worm') is used here to refer to the specific ecomorphotype characterizing the Scolecophidia *sensu lato*, also known as worm snakes. This group of worm-like organisms is morphologically and ecologically consistent. Worm snakes do indeed share a unique and very peculiar combination of attributes that led previous studies to consider them as closely related. Very likely related to an extreme degree of adaptation to fossoriality, scolecoidy is characterized by the following, nonexhaustive, combination of traits: a marked trend towards miniaturization, a body that is uniform in diameter throughout its length, covered by smooth cycloid scales, sub-equal in size and undifferentiated ventrally; a blunt head and tail, with a conical scale at the tip of the tail (Savage, 2002); highly regressed eyes (microphtalmy) fully covered by large translucent scales (brille absent), and whose retina contains only rods (Repérant *et al.*,

1992; Savage, 2002); and a diet predominantly composed of larvae and pupae of social insects (Colston *et al.*, 2010; Parpinelli & Marques, 2015). Finally, the osteological features characterizing scolecophidians *s. l.*, regarded by Kley (2006) as a '*vexing mixture of primitive and derived characters*', differ markedly from those encountered among the Alethinophidia.

2) *Visual cell patterns* [two states: *presence* versus *absence* of retinal cones]. The eyes of snakes are remarkable for being highly divergent in gross morphology from those of other squamates. They lack photoreceptor oil droplets, are covered by a transparent head scale (spectacle or brille), are lacking a sclerotic ring and present evidence for evolutionary transitions ('transmutation') between rods and cones. Remarkably, cones are absent in two groups of snakes highly adapted to burrowing life-style, in the Aniliidae and in all the species of Scolecophidia *s.l.* that have been studied (n = 5), (Simões *et al.*, 2015, 2016). It should however be emphasized that evolutionary research on the visual systems of snakes is in its infancy, and that the taxonomic sampling for which these data are available is relatively sparse (see also Schott *et al.*, 2018).

3) *Mouth anatomy* [two states: *macrostomy* versus *non-macrostomy* (=*microstomy*)]. Macrostomy corresponds to an anatomical characteristic that permits the ingestion of entire prey with a large diameter. Associated to a nonburrowing or epigean life-style, it depends on several osteological and soft tissue traits, of which the elongation of the jaw complex and the backward rotation of the quadrate represent crucial skeletal requirements (Scanferla, 2016).

Results

Phylogenetic results

Both BI and ML phylogenetic analyses provided congruent and well resolved trees, with the most basal nodes being fully supported (Fig. 1). Complementary analyses (Species tree inferred by ASTRAL and concatenated analyses excluding chimeric assemblages) result in topologies that are congruent with the two main analyses (cf. Appendix S4 and S5). All the inferred topologies congruently reject the monophyly of the Scolecophidia *sensu lato*: four families, the Gerrhopilidae (GeD), Xenotyphlopidae (XeD), Typhlopidae (TyD) and Leptotyphlopidae (LeD) cluster together (Scolecophidia *sensu stricto*), whereas the Anomalepididae are the sister clade to all the other snakes (Alethinophidia). The monophyly of Scolecophidia *sensu stricto* and of the Anomalepididae + Alethinophidia clade is fully supported by the concatenated approaches (BI: 100/ML: 1.0 for both clades). These two clades are also supported by the ST (nodes support of 0.78 and 0.86, respectively). Considering the separate analyses by

locus, these two clades have been independently retrieved by six of 14 and seven of 13 separate analyses per locus, respectively. Alternative relationships (Anomalepididae sister group to the other snakes and Anomalepididae sister group to the Scolecophidia *s.s.*) were retrieved by only three and two of 13 separate analyses, respectively (Appendix S6).

Three main subclades are recovered among the monophyletic Alethinophidia (BI: 100/ML: 1.0): (1) the Amerophidia (Aniliidae + Tropidophiidae) and (2) the Uropeltoidea (*Uropeltis*+*Cylindrophis*) are retrieved with a strong support (100/1.0 each), whereas (3) the Macrostomata clade (and also some of its most basal internal relationships) is moderately supported (60/0.94). The monophyly of Afrophidia (Uropeltoidea + Macrostomata *s.s.*) is strongly supported (99/1.0).

Within Scolecophidia *sensu stricto*, the interfamilial relationships, fully resolved and supported (100/1.0) are the following [LeD (GeD (XeD+TyD))], in agreement with the most recent studies focusing on this group (Vidal *et al.*, 2010; Hedges *et al.*, 2014; Nagy *et al.*, 2015). More specifically, within the Typhlopidae clade–for which a significant amount of new data has been generated here–the topology retrieves the monophyly of each subfamily: (1) the american Typhlopinae (TyN), with the following internal arrangement: [*Amerotyphlops* (*Cubatyphlops* (*Typhlophis* + *Antillotyphlops*))], (2) the Euraustralasian Asiatyphlopinae (AsiaN): [(*Xerotyphlops* (*Indotyphlops* ((*Anilios* + *Sundatyphlops*) (*Rhamphotyphlops* + *Malayotyphlops*)))] and (3) the african Afrotyphlopinae (AfroN): [*Afrotyphlops* (*Letheobia* + *Rhinotyphlops*)]. The monophyly of the monogeneric Malagasy Madatyphlopinae (MadaN) has not been tested here, but has already been convincingly demonstrated by Nagy *et al.* (2015). Relationships between the four Typhlopidae subfamilies are the following: [TyN (AsiaN (AfroN, MadaN)].

Dating

The estimated divergence dates are presented in Fig. 2 (see also Appendix S7 for details). Interestingly, these results are very similar to those recently published by Zheng & Wiens (2016), despite the fact that both studies are based on significantly different molecular datasets and completely different calibration points (cf. table 1). Notably, our results confirm the relatively ancient origin of the extant snakes, the four main clades–Alethinophidia Anomalepididae, Leptotyphlopidae and Typhlopoidea–having diverged from each other during the Early Cretaceous.

Ancestral state reconstruction (ASR)

The present study aims to investigate the evolutionary history of the scolecoid ecomorphotype using the newly
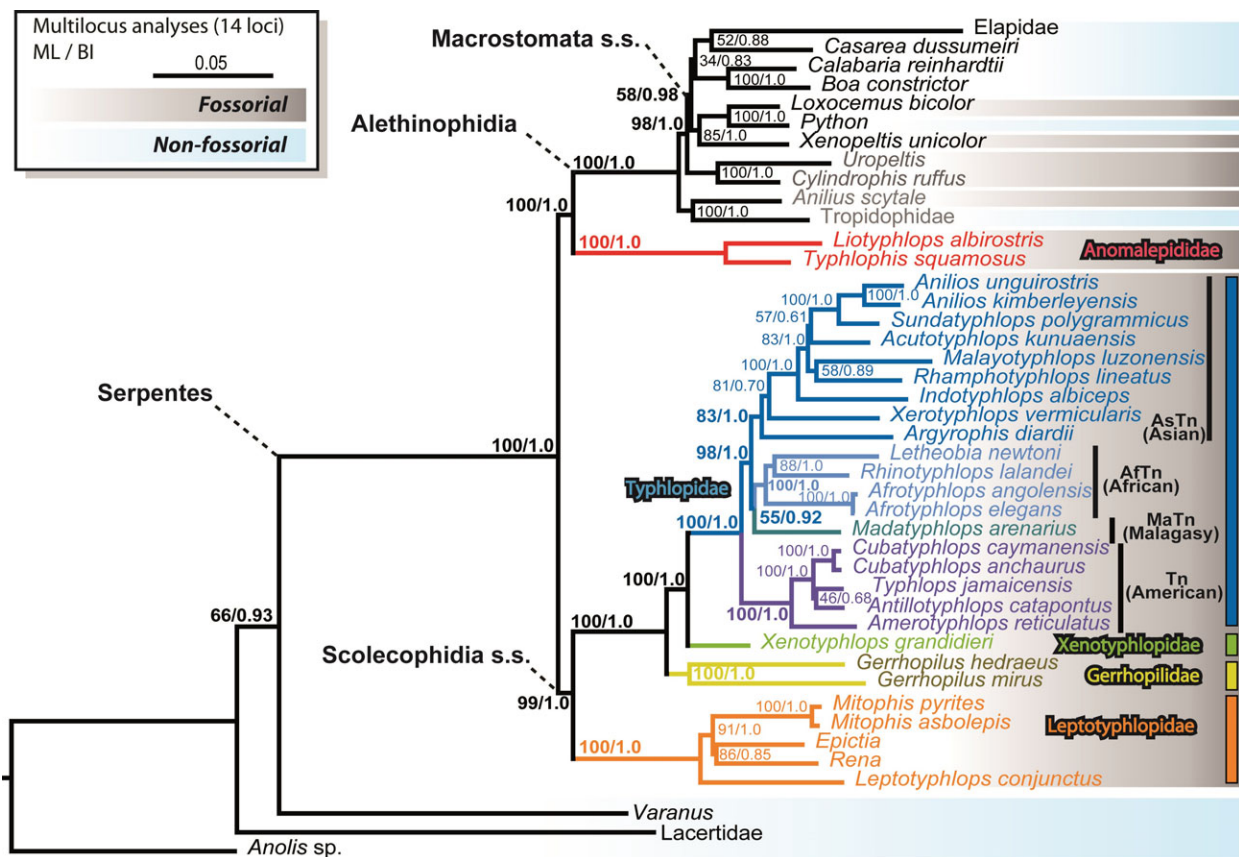
Fig. 1 Phylogenetic tree of snakes, reconstructed using maximum likelihood, based on concatenated DNA sequences of 14 nuclear loci (CAND1, CMOS, DNAH3, ENC1, SLC8A1, SNCAIP, R35, ZEB2, ZFP36, BDNF, RAG1, BMP2, NT3 and AMEL), with bootstrap support values (%), followed by the posterior probabilities from the Bayesian inference. Ecological traits are represented by colours highlighting each clade. Families of the paraphyletic Scolecophidia *sensu lato* are highlighted in bold and in colour. AsTn, AfTn, MaTn and Tn refer to the Asian (Asiotyphlopinae), African (Afrotyphlopinae), Malagasy (Madatyphlopinae) and American (Typhlopinae) clades of Typhlopidae, respectively.

inferred topology as an interpretative framework. For the sake of clarity, reconstructions have been summarized to the six main clades of snakes (Fig. 3). The inferred ASR results will only be discussed for the deepest nodes of the snake tree. The complete analyses are available in Appendix S8 and S9:

Scolecoidy ASR
Both the ML- and BI-ASR strongly support scolecoidy as the ancestral state for extant snakes, subsequently lost in the Alethinophidia (Fig. 3a). The MP reconstruction is ambiguous for the two most basal nodes, involving two equally parsimonious scenarios (scolecoidy being either a plesiomorphic state, congruently with ML and BI reconstructions, or convergently appearing in the Scolecophidia *sensu stricto* and the Anomalepididae). The state inferred for all the other main nodes are unambiguous, and fully congruent among the four approaches.

Visual cells patterns ASR
According to both the ML- BI-ASR, the absence of cones would more likely constitute the ancestral state of extant snakes, the cones having reappeared in Alethinophidia (then would have subsequently been lost in the Aniliidae; Fig. 3b). The MP-ASR is relatively uninformative given that the most basal nodes of the snake tree are not resolved, but all the resolved nodes are nevertheless fully congruent with both the ML and BI inferences.

Mouth anatomy ASR
The MP-, ML- and BI-ASR inferences all congruently support the microstomy in Anomalepididae and Scolecophidia *sensu stricto* as a plesiomorphic state inherited from the common ancestor of extant snakes (Fig. 3c). They nevertheless provide contrasting scenarios concerning the origin of macrostomy: the ML reconstruction supports a single change towards macrostomy with
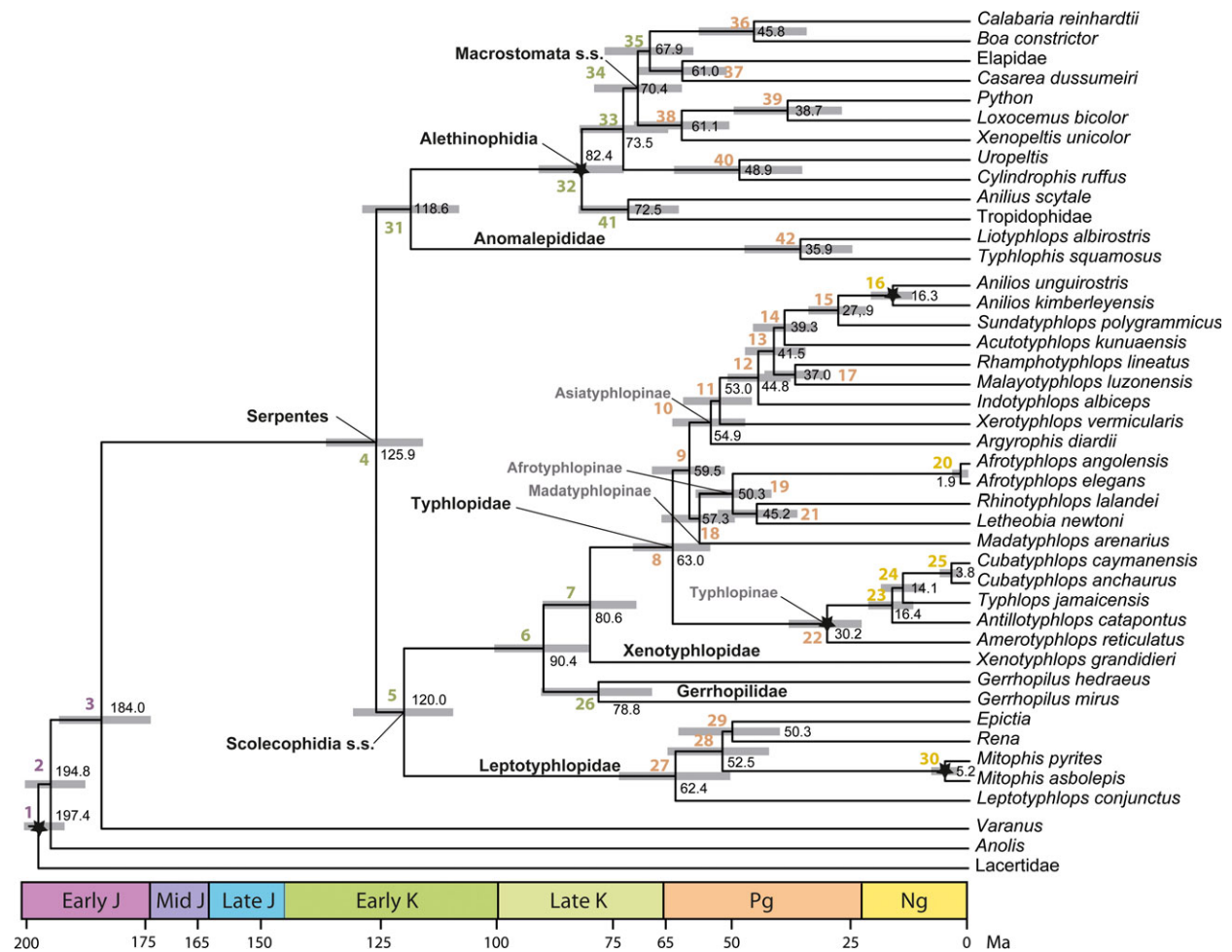
Fig. 2 Divergence time tree inferred with BEAST. Grey bars at nodes indicate 95% credibility intervals for divergence events. Temporal scale is shown in millions of years. The five calibration point used to estimate node ages are represented by black stars. Node numbers are represented in bold and in colour and node ages in black (see details in Appendix S7).

two independent subsequent reversions towards microstomy in both Uropeltoideae and Aniliidae, whereas the MP and BI reconstruction congruently supports two distinct changes towards a derived macrostomy in Macrostomata s. s. and in Tropidophiidae.

Additionally, the analyses based on BT-ASR (which take into account topological uncertainty) support the hypothesis according to which the last common ancestor of the extant snakes would have been characterized by traits associated with fossorial organism (scolecoid morphotype, with no retinal cones and a microstomate anatomy). In contrast, these analyses mostly differed from the fixed-topology ASR by providing ambiguous or contradictory results for the common ancestor of the Anomalepididae and the Alethinophidia, suggesting that the 'scolecoid' traits characterizing both the Anomalepidae and the Scolecophidia s.s. might result from convergent evolution.

Discussion

Deep phylogenetic relationships among Typhlopidae

The generic relationships of Typhlopidae inferred from our extended dataset differ from those published recently (Hedges *et al.*, 2014; Pyron & Wallach, 2014; Nagy *et al.*, 2015) by presenting a better resolution and a stronger support of the basal most nodes, offering a relatively clear understanding of the inter-subfamilial relationships (Fig. 1). Notably, the Typhlopinae (American clade) is retrieved as sister clade with respect to the other subfamilies—instead of the Asiatyphlopinae (Asian clade) as was previously obtained (with low support) by Hedges *et al.* (2014) and Pyron & Wallach (2014). Madatyphlopinae are also retrieved for the first time as sister clade of the Afrotyphlopinae. Despite the fact that this 'Afro-Malagasy' clade is moderately

Table 1 Comparison of the estimated divergence dates for the main clades of snakes obtained in the present study with those obtained by Zheng & Wiens (2016). Node numbers refer to those presented in fig. 2.

Nodes	Zheng & Wiens, 2016	Present study
Serpentes [4]	128.1	125.9 (116.2–135.9)
Scolecophidia s.s.. [5]	122.7	120.0 (110.0–130.4)
Gerrhopilidae vs. sister clade [6]	89.0	90.4 (80.8–100.5)
Xenotyphlopidae vs. Typhlopidae [7]	85.4	80.6 (71.1–90.2)
Typhlopidae [8]	70.6	63.0 (55.5–71.0)
Anomalepididae vs. Alethinophidia [31]	124.7	118.6 (108.8–128.5)
Alethinophidia (Afrophidia vs. Amerophidia) [32]	92.7	82.4 (73.9–91.1)
Aniliidae vs. Tropidophiidae [41]	79.81	72.5 (62.2–82.6)

Divergence estimates in millions of years, followed by 95% HPD intervals (HPD intervals only available for the present study).

supported by our data (68%/0.85), such a phylogenetic hypothesis is likely from a biogeographic point of view. This hypothesis is also supported by the molecular dating, which inferred a divergence between Madatyphlopinae and Afrotyphlopinae around 57.3 Mya (95% HPD interval 50.2-65.0), a period around which the multiple colonisation events of vertebrates from Africa towards Madagascar took place (70-50 My, Crottini *et al.*, 2012).

Whereas the internal topology among the Afrotyphlopinae and the Typhlopinae is fully congruent with previous studies, the basal most relationships among the Asiatyphlopinae (relative positions of *Malayotyphlops*, *Indotyphlops*, *Xerotyphlops* and *Argyrophis*) are significantly different. The support obtained for these particular relationships is relatively variable and sometimes relatively weak, which leads us to consider that additional studies will be necessary to satisfactorily resolve the relationships between these four genera. In contrast, all the other intra-subfamilial relationships appear to be well supported and are congruent with other recent studies. Biogeographic inferences from our timetree are similar to those presented in Vidal *et al.* (2010).

Paraphyletic distribution of the scolecoid ecomorphotype

Phylogenetic relationships between (1) Scolecophidia *s.s.*, (2) Anomalepididae (traditionally regarded as an additional family of Scolecophidia) and (3) Alethinophidia correspond to the two deepest cladogenetic events of the extant snakes tree topology. The resolution of this trichotomy is therefore fundamental to correctly infer attributes of the common ancestor of snakes and

to elucidate the origins of this successful radiation. Until now, no consensus on this specific question had been reached with all the three possible permutations having been alternatively retrieved by the different molecular studies published to date (cf. Fig. 4 for a comparison of the most recent topologies recovered by Pyron *et al.* (2013), Figueroa *et al.* (2016), Reeder *et al.* (2015), Streicher & Wiens (2016), Zheng & Wiens (2016), Hsiang *et al.* (2015) and Harrington & Reeder (2017).

Our results support the paraphyly of Scolecophidia *sensu lato*, with the Anomalepididae being placed as sister clade to the Alethinophidia. The latter grouping received maximal support values (100%/1.0) and has been congruently retrieved by the ST and a majority of independent lines of evidence (7/13 separated analyses per locus, see also appendix S4 and S6). These results provide a better support in comparison with recent studies having suggested the same relationship (Reeder *et al.* (2015) and Zheng & Wiens (2016) obtained scores of 50% and 95% for this node, respectively).

This topology is remarkable in the sense that it leads to a reinterpretation of the evolutionary history of the very peculiar *scolecoid* [= worm-like] ecomorphotype proper to the Scolecophidia *s.s.* and the Anomalepididae. Many of the osteological and ecological traits associated with scolecoidy have indeed been regarded as extremely derived, and therefore interpreted as synapomorphies in favour of the monophyly of the Scolecophidia *sensu lato* (e.g. Lee & Scanlon, 2002; Palci *et al.*, 2013; Hsiang *et al.*, 2015). In contrast, the ancestral state reconstructions of this ecomorphotype based on our new topology unambiguously reject such an evolutionary scenario. They rather suggest that this trait may represent an ancestral state already present at the origin of the extant snakes, subsequently regressed in the Alethinophidia. The two complementary ASR based on specific traits characterizing the 'scolecoid' state (rather than a holistic approach considering this ecomorphotype as a whole) provided results potentially congruent with an ancestral nature of the scolecoid morphotype. Both the absence of cones and the microstomy were indeed inferred as plesiomorphic traits inherited from the ancestor of extant snakes. The results obtained for the visual pattern ASR coincide with the fact that all snakes share highly derived eye anatomical traits, which is interesting because these characteristics are typically considered to reflect a burrowing origin (i.e. absence of eyelids or sclerotic ring, Underwood, 1970).

Although our results have to be considered with caution given the relatively low number of strictly fossorial clades connected at the base of the snake tree, they are overall compatible with the hypothesis according to which worm snakes might represent a very ancient phenotype inherited from the last common ancestor of extant snakes. Our results are also compatible with those published in a recent study integrating multiple
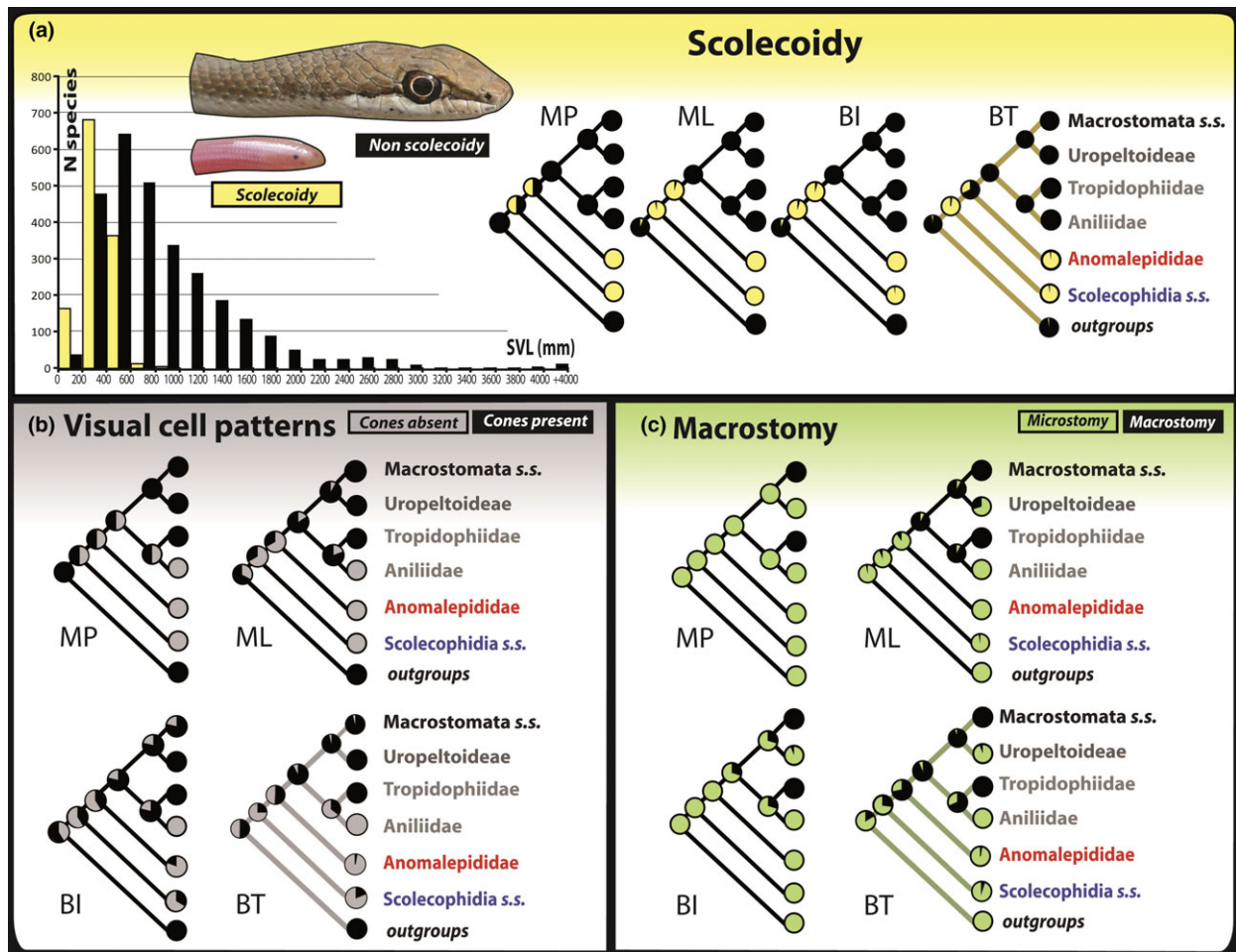
Fig. 3 Summarized ancestral state reconstructions (MP-, ML-, BI- and BT-ASR) applied to three features expected to be related to an extreme burrowing life-style: (a) Morphotype '(*scolecoidy* versus *nonscolecoidy*)', the right figure showing the miniaturization trend observed within the scolecophidians *sensu lato* (Scolecophidia *s.s.* and Anomalepididae), compared to other snakes (Alethinophia) –maximal known snout vent length of 4127 species of snakes, based on the dataset published by Feldman *et al.*, 2016; (b) visual cell pattern (*presence* versus *absence of retinal cones);* (c) cranial anatomy (*macrostomy* versus *microstomy*. Ancestral states presented for each terminal taxon (here supraspecific) correspond to the results inferred for each of their respective common ancestors (See Appendix S8, S9 and S10 for details). Photographic illustrations: *Psammophis schokari* above and *Madatyphlops arenarius* below (A. Miralles).

approaches (ecology, palaeontology, development) in order to build models of skull shape changes in squamates (Da Silva *et al.*, 2018). This recent work–which also considered the paraphyly of scolecoid snakes as a working hypothesis–revealed that the most recent common ancestor of crown snakes likely had a small skull with a shape undeniably adapted for fossoriality, whereas all snakes plus their sister group derive from a surface-terrestrial form. More interestingly, the phylomorphospace analysis provided by Da Silva *et al.* (2018) indicates that worm snakes radiated from a less-specialized (although fossorial) skull shape, suggesting that these snakes are probably not ideal in representing the skull condition of the last common ancestor of extant snakes. Nevertheless, their skull shape appears to be closer to the hypothetical ancestral snake skull than any other species of snake. In other words, several lines of evidence support the hypothesis according to which the fossoriality of both scolecophidians. *s.s.*. and Anomalepididae might be fundamentally plesiomorphic, and that it might have persisted only in these two taxa since the primordial incursion of snakes towards an underground environment.

Acknowledgments
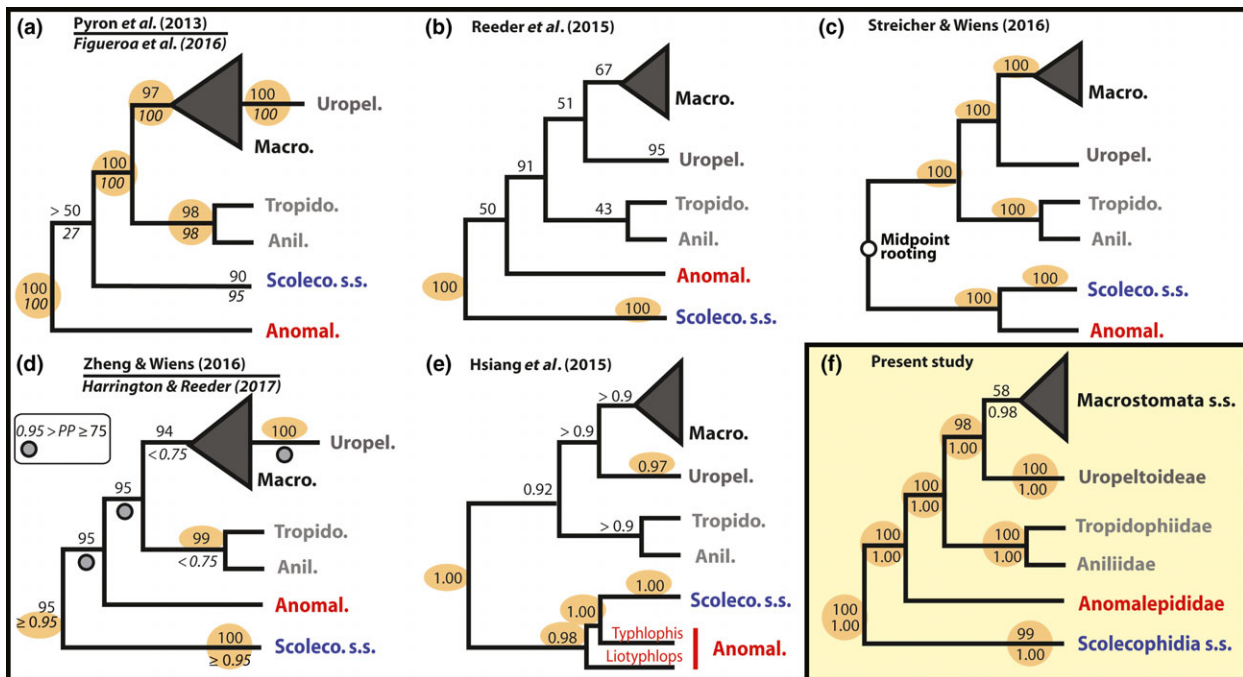
Fig. 4 Alternative hypotheses on the evolution of snakes. Simplified topologies of recently published higher-level snake phylogenies are compared with the results obtained in the present study (F), ML bootstraps scores and BI PP indicated above and below each nodes, respectively: (a) Pyron *et al.* (2013)/Figueroa *et al.* (2016: fig. 1), both ML, with SHL (nonparametric Shimodaira-Hasegawa-Like test) scores; (b) Reeder *et al.* (2015: fig. 1), ML with bootstrap scores; (c) Streicher & Wiens (2016: fig. 4A), ML with bootstrap scores; (d) Zheng & Wiens (2016: fig. 1), ML with bootstrap scores/Harrington & Reeder (2017: fig 2), preferred BI (PP support only represented by intervals in the original article); (e) Hsiang *et al.* (2015: fig. 3), BI combining morphological and genetic datasets, with PP scores.) Nodes strongly supported (ML Bootstraps, SHL or PP scores > 95%) are highlighted by orange circles.

References

Adalsteinsson, S.A., Branch, W.R., Trape, S., Vitt, L.J. & Hedges, S.B. 2009. Molecular phylogeny, classification, and biogeography of snakes of the Family Leptotyphlopidae (Reptilia, Squamata). *Zootaxa* **2244**: 1–50.

Bouckaert, R., Heled, J., Kühnert, D., Vaughan, T., Wu, C.-H., Xie, D. *et al.* 2014. BEAST 2: a software platform for bayesian evolutionary analysis. *PLoS Comput. Biol.* **10**: e1003537.

Colston, T.J., Costa, G.C. & Vitt, L.J. 2010. Snake diets and the deep history hypothesis. *Biol. J. Linnean Soc.* **101**: 476–486.

Crottini, A., Madsen, O., Poux, C., Strauss, A., Vieites, D.R. & Vences, M. 2012. Vertebrate time-tree elucidates the biogeographic pattern of a major biotic change around the K-T boundary in Madagascar. *Proc. Natl Acad. Sci. USA* **109**: 5358–5363. https://doi.org/10.1073/pnas.1112487109.

Cundall, D. & Greene, H.W. 2000. 2000. Feeding in snakes. In: *Feeding, form, function, and evolution in tetrapod vertebrates* (K. Schwenk, ed), pp. 293–333. Academic Press, San Diego.

Da Silva, F.O., Fabre, A.-C., Savriama, Y., Ollonen, J., Mahlow, K., Herrel, A. *et al.* 2018. The ecological origins of snakes as revealed by skull evolution. *Nat. Commun.* **9**: 376.

Drummond, A.J., Suchard, M.A., Xie, D. & Rambaut, A. 2012. Bayesian phylogenetics with BEAUti and the BEAST 1.7. *Mol. Biol. Evol.* **29**: 1969–1973. https://doi.org/10.1093/molbev/mss075.

Feldman, A., Sabath, N., Pyron, R.A., Mayrose, I. & Meiri, S. 2016. Body-sizes and diversificiation rates of lizards, snakes, amphisbaenians and tuatara. *Global Ecol. Biogeogr.* **25**: https://doi.org/10.1111/geb.12398.

Figueroa, A., McKelvy, A.D., Grismer, L.L., Bell, C.D. & Lailvaux, S.P. 2016. A species-level phylogeny of extant snakes with description of a new colubrid subfamily and genus. *PLoS ONE* **11**: e0161070.

Greene, H.W. 1997. *Snakes: the evolution of mystery in nature*, p. 351. University of California Press, Berkeley, California.

Harrington, S.M. & Reeder, T.W. 2017. Phylogenetic inference and divergence dating of snakes using molecules, morphology and fossils: new insights into convergent evolution of feeding morphology and limb reduction. *Biol. J. Linn. Soc.* **121**: 379–394.

Hedges, S.B., Marion, A.B., Lipp, K.M., Marin, J. & Vidal, N. 2014. A taxonomic framework for typhlopid snakes from the Caribbean and other regions (Reptilia, Squamata). *Carib. Herpet.* **49**: 1–61.

Hsiang, A.Y., Field, D.J., Webster, T.H., Behlke, A.D.B., Davis, M.B., Racicot, R.A. *et al.* 2015. The origin of snakes:

revealing the ecology, behavior, and evolutionary history of early snakes using genomics, phenomics, and the fossil record. *BMC Evol. Biol.* **15**: 87. https://doi.org/10.1186/s12862-015-0358-5.

Huebeck, C. & Mann, P. 1985. Structural geology and Cenozoic tectonic history of the southeastern termination of the Cordillera Central, Dominican republic. *Geol. Soc. Am. Spec. Pap.* **262**: 315–336.

Iturralde-Vinent, M.A. & MacPhee, R.D.E. 1999. Paleogeography of the Caribbean region: implications for the Cenozoic biogeography. *Bull. Am. Mus. Nat. Hist.* **238**: 1–95.

Kley, N.J. 2006. Morphology of the lower jaw and suspensorium in the Texas blindsnake, *Leptotyphlops dulcis* (Scolecophidia: Leptotyphlopidae). *J. Morphol.* **267**: 494–515.

Kumar, S., Stecher, G. & Tamura, K. 2016. MEGA7: molecular Evolutionary Genetics Analysis version 7.0. for bigger datasets *Mol. Biol. Evol.* **33**: 1870–1874.

Lanfear, R., Frandsen, P.B., Wright, A.M., Senfeld, T. & Calcott, B. 2016. PartitionFinder 2: new methods for selecting partitioned models of evolution for molecular and morphological phylogenetic analyses. *Mol. Biol. Evol.*. https://doi.org/dx.doi.org/10.1093/molbev/msw260.

Lee, M.S. & Scanlon, J.D. 2002. Snake phylogeny based on osteology, soft anatomy and ecology. *Biol. Rev. Camb. Philos. Soc.* **77**: 333–401.

Li, B. & Lecointre, G. 2009. Formalizing reliability in the taxonomic congruence approach. *Zool. Scripta* **38**: 101–112.

Longrich, N.R., Bhullar, B.-A.S. & Gauthier, J.A. 2012. A transitional snake from the late cretaceous period of North America. *Nature* **488**: 205–208.

Maddison, W.P. & Maddison, D.R. 2016. Mesquite: a modular system for evolutionary analysis. Version 3.11. http://mesquiteproject.org

Marin, J., Donnellan, S.C., Hedges, S.B., Puillandre, N., Aplin, K.P., Doughty, P. *et al.* 2013. Hidden species diversity of Australian burrowing snakes (*Ramphotyphlops*). *Biol. J. Linn. Soc.* **110**: 427–441.

McDiarmid, R.W., Campbell, J.A. & Touré, T. 1999. Snake Species of the World: A Taxonomic and Geographic Reference, vol. 1. Herpetologists' League. 511 pp.

Miller, M. A., Pfeiffer, W. & Schwartz, T. 2010. "Creating the CIPRES Science Gateway for inference of large phylogenetic trees" in Proceedings of the Gateway Computing Environments Workshop (GCE), 14 Nov. 2010, New Orleans, LA pp 1 – 8

Mirarab, S., Reaz, R., Bayzid, M.S., Zimmermann, T., Swenson, M.S. & Warnow, T. 2014. ASTRAL: genome-scale coalescent-based species tree estimation. *Bioinformatics* **30**: i541–i548.

Nagy, Z.T., Marion, A.B., Glaw, F., Miralles, A., Noppers, J., Vences, M. *et al.* 2015. Molecular systematics and undescribed diversity of Madagascan scolecophidian snakes (Squamata: serpentes). *Zootaxa* **4040**: 31–47.

Pagel, M. & Meade, A. 2006. Bayesian analysis of correlated evolution of discrete characters by reversible-jump Markov chain Monte Carlo. *Am. Nat.* **167**: 808–825.

Pagel, M., Meade, A. & Barker, D. 2004. Bayesian estimation of ancestral character states on phylogenies. *Syst. Biol.* **53**: 673–684.

Palci, A., Caldwell, M.W. & Albino, A.M. 2013. Emended diagnosis and phylogenetic relationships of the upper cretaceous fossil snake *Najash rionegrina* apesteguía and zaher, 2006. *J. Vert. Paleontol.* **33**: 131–140.

Parpinelli, L. & Marques, O.A.V. 2015. Reproductive biology and food habits of the Blindsnake *Liotyphlops beui* (Scolecophidia: Anomalepididae). *S. Am. J. Herpetol.* **10**: 205–210.

Poux, C., Chevret, P., Huchon, D., de Jong, W.W. & Douzery, E.J. 2006. Arrival and diversification of caviomorph rodents and platyrrhine primates in South America. *Syst. Biol.* **55**: 228–244.

Pyron, R.A. & Wallach, V. 2014. Systematics of the blindsnakes (Serpentes: Scolecophidia: Typhlopoidea) based on molecular and morphological evidence. *Zootaxa* **3829**: 001–081.

Pyron, R.A., Burbrink, F.T. & Wiens, J.J. 2013. A phylogeny and revised classification of Squamata, including 4161 species of lizards and snakes. *BMC Evol. Biol.* **13**: 93.

Rambaut, A., Suchard, M.A., Xie, D. & Drummond, A.J. 2014. Tracer v1.6, Available from http://beast.bio.ed.ac.uk/Tracer

Reeder, T.W., Townsend, T.M., Mulcahy, D.G., Noonan, B.P., Wood, P.L. Jr, Sites, J.W. Jr *et al.* 2015. Integrated analyses resolve conflicts over squamate reptile phylogeny and reveal unexpected placements for fossil taxa. *PLoS ONE* **10**: e0118199.

Repérant, J., Rio, J.-P., Ward, R., Hergueta, S., Miceli, D. & Lemire, M. 1992. Comparative analysis of the primary visual system of reptiles. In: *Sensory Integration. Biology of Reptilia Vol.17, Neurology C, Chapter: 3* (C. Gans & P. S. Ulinski, eds), pp. 175–240. The University of Chicago Press, Chicago, London.

Rieppel, O., Kluge, A.G. & Zaher, H. 2002. Testing the phylogenetic relationships of the Pleistocene snake *Wonambi naracoortensis* Smith. *J. Vert. Paleontol.* **22**: 812–829.

Ronquist, F. & Huelsenbeck, J.P. 2003. MrBayes 3: bayesian phylogenetic inference under mixed models. *Bioinformatics* **19**: 1572–1574.

Savage, J.M. 2002. *The amphibians and reptiles of costa rica: a herpetofauna between two continents*, p. 934. University of Chicago Press, Chicago and London, Between Two Seas.

Sayyari, E. & Mirarab, S. 2016. Fast coalescent-based computation of local branch support from quartet frequencies. *Mol. Biol. Evol.* **33**: 1654–1668.

Scanferla, A. 2016. Postnatal ontogeny and the evolution of macrostomy in snakes. *R. Soc. Open Sci.* **3**: 160612.

Schott, R.K., Van Nynatten, A., Card, D.C., Castoe, T.A. & Chang, B.S.W. 2018. Shifts in selective pressures on snake phototransduction genes associated with photoreceptor transmutation and dim-light ancestry. *Mol. Biol. Evol.* **35**: 1376–1389.

Simões, B.F., Sampaio, F.L., Jared, C., Antoniazzi, M.M., Loew, E.R., Bowmaker, J.K. *et al.* 2015. Visual system evolution and the nature of the ancestral snake. *J. Evol. Biol.* **28**: 1309–1320. https://doi.org/10.1111/jeb.12663.

Simões, B.F., Sampaio, F.L., Douglas, R.H., Kodandaramaiah, U., Casewell, N.R., Harrison, R.A. *et al.* 2016. Visual pigments, ocular filters and the evolution of snake vision. *Mol. Biol. Evol.* **33**: 2483–2495.

Springer, M.S., Scally, M., Madsen, O., de Jong, W.W., Douady, C.J. & Stanhope, M.J. 2004. The use of composite taxa in supermatrices. *Mol. Phylogenet. Evol.* **30**: 883–884.

Stamatakis, A. 2014. RAxML Version 8: a tool for phylogenetic analysis and post-analysis of large phylogenies. *Bioinformatics* **30**: 1312–1313.

Streicher, J.W. & Wiens, J.J. 2016. Phylogenomic analyses reveal novel relationships among snake families. *Mol.*

Phylogenet. Evol. **100**: 160–169. https://doi.org/10.1016/j.ympev.2016.04.015.

Talavera, G. & Castresana, J. 2007. Improvement of phylogenies after removing divergent and ambiguously aligned blocks from protein sequence alignments. *Syst. Biol.* **56**: 564–577.

Uetz, P., Freed, P. & Hošek, J. (eds.), The Reptile Database, http://www.reptile-database.org, accessed February 2018.

Underwood, G. 1970. The eye. In: *Biology of the Reptilia, Morphology B*, vol. **2** (C. Gans, T.S. Parsons, eds), pp. 1–97. Academic Press, New York.

Vidal, N. & Hedges, S.B. 2002. Higher-level relationships of snakes inferred from four nuclear and mitochondrial genes. *C. R. Biologies* **325**: 977–985.

Vidal, N. & Hedges, S.B. 2005. The phylogeny of squamate reptiles (lizards, snakes, and amphisbaenians) inferred from nine nuclear protein-coding genes. *C. R. Biologies* **328**: 1000–1008.

Vidal, N., Rage, J.-C., Couloux, A. & Hedges, S.B. 2009. Snakes (Serpentes). In: *The timetree of life* (S.B. Hedges, S. Kumar, eds), pp. 390–397. Oxford University Press, New York, NY.

Vidal, N., Marin, J., Morini, M., Donnellan, S., Branch, W.R., Thomas, R. *et al.* 2010. Blindsnake evolutionary tree reveals long history on Gondwana. *Biol. Lett.* **6**: 558–561.

Wiens, J.J., Hutter, C.R., Mulcahy, D.G., Noonan, B.P., Townsend, T.M., Sites, J.W. Jr *et al.* 2012. Resolving the phylogeny of lizards and snakes (Squamata) with extensive sampling of genes and species. *Biol. Lett.* **8**: 1043–1046.

Zheng, Y. & Wiens, J.J. 2016. Combining phylogenomic and supermatrix approaches, and a time-calibrated phylogeny for squamate reptiles (lizards and snakes) based on 52 genes and 4162 species. *Mol. Phylogenet. Evol.* **94**: 537–547.

Supporting information

Additional supporting information may be found online in the Supporting Information section at the end of the article.

Appendix S1 List of samples and accession numbers of the sequences with their references and localities.

Appendix S2 List of primers and PCR conditions.

Appendix S3 Character states used in the ASR.

Appendix S4 Species tree inferred by ASTRAL.

Appendix S5 Phylogenetic tree restricted to strictly specific terminal taxa (chimeric assemblages excluded).

Appendix S6 Fourteen separated ML analyses (per loci)

Appendix S7 Time tree analysis.

Appendix S8 Ancestral state reconstructions.

Appendix S9 Ancestral state reconstructions taking into account incertainty.

Appendix S10 Miniaturization trend observed within the two "scolecophidian" clades (Scolecophidia s.s. and Anomalepididae), compared with the other three main clades of non-scolecophidian snakes.